

XMM Flight Model Mirror Module Testing

Y. Stockman, P. Barzin, H. Hansen, E. Mazy, J. Ph. Tock
CSL – University of Liège
B- 4031 Angleur, Belgium
email : ystockman@ulg.ac.be

D. de Chambure, R. Lainé
ESA / ESTEC
PO BOX 299, 2200 AG Noordwijk, The Netherlands

D. Kampf
Kayser Threde
Wolfratshauser Str., 48,
D-81379 Munich, Germany

R. Banham, M. Canali, G. Grisoni, P. Radaelli
Media Lario, Località Pascolo
I-23842 Bosisio Parini (LC), Italy

ABSTRACT

In the frame of the X-ray Multi Mirror Mission (XMM), the second European Space Agency (ESA) cornerstone project, in total five Flight Models of the Mirror Module have been built. The Mirror Modules are the optical heart of the satellite. Each Mirror Module contains 58 X-ray optical quality Mirror Shells which have been produced and integrated by Media Lario. Each of these Mirror Modules has been tested in the Centre Spatial de Liège (CSL) FOCAL-X facility. The goal of these tests was to measure the optical performance of the Mirror Modules under simulated launch and in-orbit configurations, and to perform some calibration on the Mirror Modules. To achieve these goals, a full EUV (58.4 nm) collimated beam is used to assess the optical characteristic in a representative flight configuration. The X-ray performance is controlled by means of an X-ray pencil beam and an X-ray collimator. The pencil beam is used for the determination of the Mirror Shell position, wing scattering and X-ray reflectivity measurements, the later one for the effective area measurement over 1.5 to 8 keV energy range.

This paper mainly deals with the latest results achieved on the Flight Model 4 Mirror Assembly and the fifth Flight Mirror Module. The first one is integrated on the spacecraft, the second has been built to serve as an additional spare flight MM of the highest quality and to further develop the mirror module production and measurement process.

After the presentation of these test results, the lessons learnt from the manufacturing and the testing of the mirrors will be presented.

KEYWORDS:

X-ray optics and telescope, EUV optics, test facility, XMM.

1. INTRODUCTION

By the end of 1999, the X-ray Multi-Mirror Mission (XMM)¹ will be launched on an Ariane V rocket. XMM is an observatory mission that will operate in the 0.1 to 10 keV range of the electromagnetic spectrum. It is the largest scientific instrument ever built by ESA. Due to its exceptional large collecting area, it will provide unprecedented observation of X-ray sources.

To meet this unique challenge, the optical heart of the mission² consists of 3 Mirror Assemblies (MA). Each MA includes a Mirror Module (MM) containing 58 electroformed X-ray quality Mirror Shells (MS) and X-ray and optical baffle (XRB and entrance baffle) to reduce stray light. Two of the three MA are equipped with a Reflection Grating Assembly (RGA) for spectral analysis.

Between 1996 and 1999, a total of nine MMs (1 QM, 3 STM and 5 FM) have been built at Media Lario. Each of these MM has been extensively tested in the Centre Spatial de Liège (CSL)³ facilities. These tests are required to:

- ☞ make a first assessment of the image quality of the MMs in a configuration as close as possible to the in-orbit operation,
- ☞ verify that the launch and the thermal space environment do not degrade the Mirror Assembly in terms of mechanical integrity and optical performance,
- ☞ check that the X-ray Baffles (XRB) and Reflection Grating Assembly (RGA) are correctly designed, integrated and aligned on the MMs.

Each of these goals has been fulfilled.

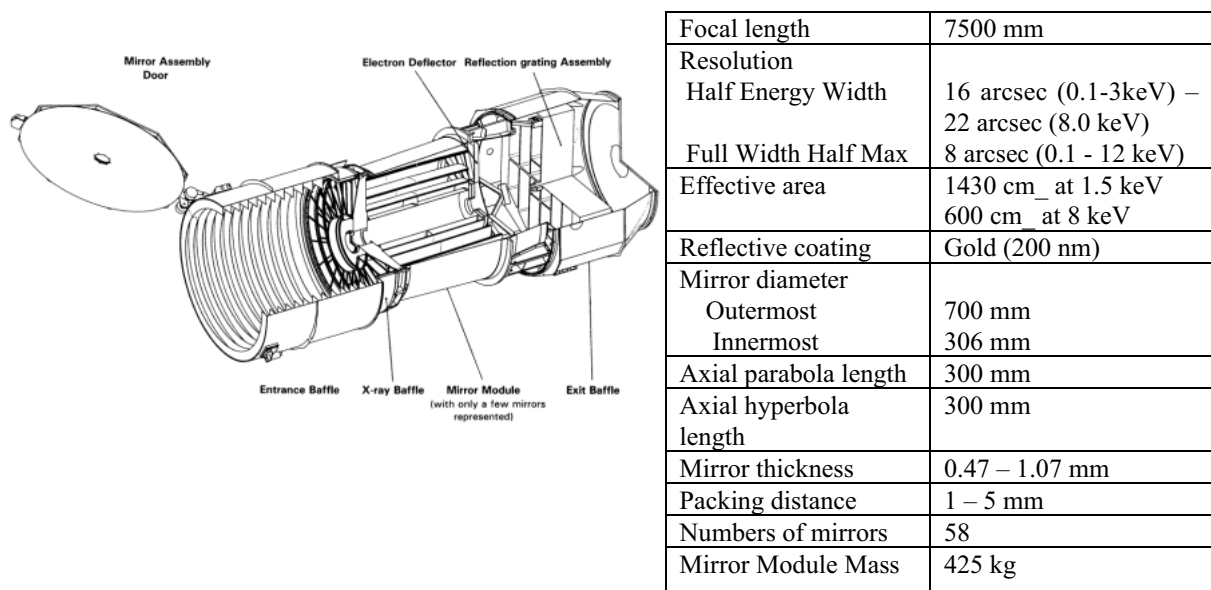
This paper will briefly describe an XMM MM and will present the final experimental results achieved on the MM FM4 + RGA1. This is the last actual flight configuration calibrated at CSL. At the beginning of 1999 the last flight model, FM5 has been delivered to ESA and tested at CSL. This MM is significant to the XMM program not only as a flight quality spare module, but has also made possible further optimisation of the mirror production and integration technique developed during the programme. In the frame of the test programme it has also been possible to make a dedicated test to cross correlate the optical measurements made by Media Lario during the MM manufacturing and integration with the CSL results. This has enabled a further understanding of the image quality of an individual Mirror Shell (MS) with respect to the final Mirror Module performance. The results and analysis of these tests are presented.

2. XMM MIRROR MODULE DESCRIPTION

The tested specimens used are the XMM Flight Model Mirror Module², as shown in figure 1. This is a Wolter I grazing incidence telescope with a focal length of 7.5 m optimised to work in the 0.1 to 12 keV energy band with a spatial resolution of 22 arcsec at 8.0 keV. One Mirror Module contains 58-nested Wolter I mirrors assembled in a close packed, nested arrangement and glued at one end only to a sixteen spoked structure known as “Spider”. During the integration process the mirrors are co-aligned and co-focused by means of a Vertical Optical Bench (VOB) that uses a collimated 633nm laser source. After completion of the mirror integration the spider is attached to the Mirror Interface Structure (MIS) that is bolted to the spacecraft platform. In front of this spider, 85mm away, an X-ray baffle⁷ is positioned to reduce stray light from sources slightly outside the Field Of View (FOV). The baffle consists of a series of “sieve plates”, made out of circular strips. These plates are aligned with the front edge of the mirrors, in order to block the single hyperbola reflected rays without vignetting the double-reflected rays. The RGA is placed 500 mm behind the mirrors. It consists of a Beryllium structure holding about 200 identical diffraction gratings. Each of these gratings is 10 cm by 20 cm square size and is oriented so that the diffracted beams intersect at a common point on the Rowland circle.

All the Mirror Modules have been subjected to an acceptance and qualification test programme at CSL⁸. X-ray calibration tests were performed at the MPE.

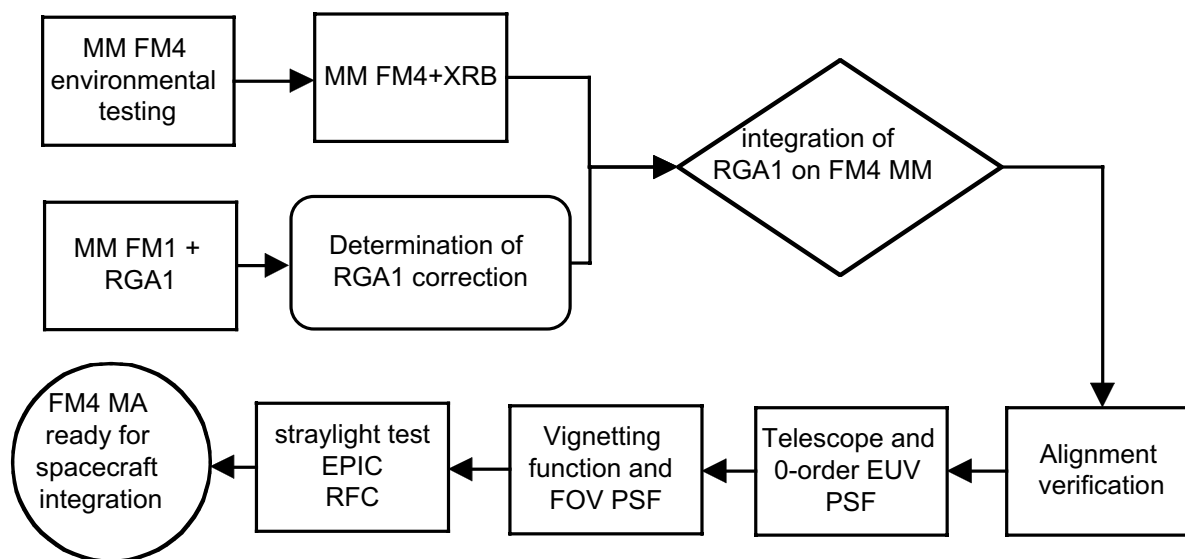
Figure 1. : Design of an XMM MA and main specifications of a MM



3. TESTING OF MM FM4 WITH RGA1

The test plan of the MM FM4 + RGA1 is presented in the flow chart of figure 2. The RGA1 has been tested first with the FM1 MM⁶. During the verification tests of the orientation of the RGA1 with respect to the MM, it was confirmed that the RGA1 had to be tilted slightly with respect to the MM due to the mounting of the gratings. This correction has been performed by changing the Titanium interface feet size. The FM4 MM has followed the standard acceptance tests. The RGA1 and the Exit Baffle are now finally integrated on the FM4 MM for final testing. After this integration no modification is allowed, and the MA is integrated on the spacecraft.

Figure 2. FM4 MA CSL test flow chart



The performance of the MA is influenced by the alignment of the RGA1 with respect to the MM FM4. This was controlled by measuring the EUV collimator axis with respect to gravity axis using the RGA itself. The method uses the measured distance between the telescope and the 0 order foci for four different orientations at 90 degrees from each other. These rotations are performed around the gravity axis. This is controlled via electronic level. The achieved value is compared to the EUV collimator optical axis measured with a liquid mirror and a theodolite, a difference of about 20 arcsec is observed. This is within the measurement accuracy and repeatable to better than 3 arcsec in both directions. The differences with respect to FM3 MM + RGA2 are less than 8 arcsec which confirm that the RGA1 is correctly integrated.

The impact of RGA1 integration on the Point Spread Function (PSF) at telescope focus is evaluated by comparing images taken with and without RGA. The images are taken at a wavelength of 30.3 nm in order to decrease the diffraction contribution (figure 3). The integration of the RGA1 enhanced the triangular shape however this has no significant impact on the HEW inside the measurement accuracy and is 14 arcsec.

Other parameters were checked (e.g.; astigmatism, vignetting function, extra-focal images, image quality in the FOV) and confirm good correlation with the predicted results.

The Focal X facility has been designed to allow several kinds of stray light tests from small angle (a few arcmin) up to 7 arc degrees. These measurements are performed⁵ by tilting the optical bench (on which the MM is fixed) with respect to the optical stimuli axis. Stray light measurement in EPIC area for angle between 20 to 90 arcmin by steps of 10 arcmin, 3, 5 and 7 degrees for 2 orthogonal azimuths has been made. The results are similar to the one achieved with RGA2 + FM3 MM. For the EPIC camera, the images are a composite of nine EUV CCD images. The energy of these images is evaluated to calculate the stray light contribution in term of effective area. The same images and numerical results are observed as for the other MA combination with RGA2⁶.

Figure 3.a : EUV PSF at 30.4 nm without RGA

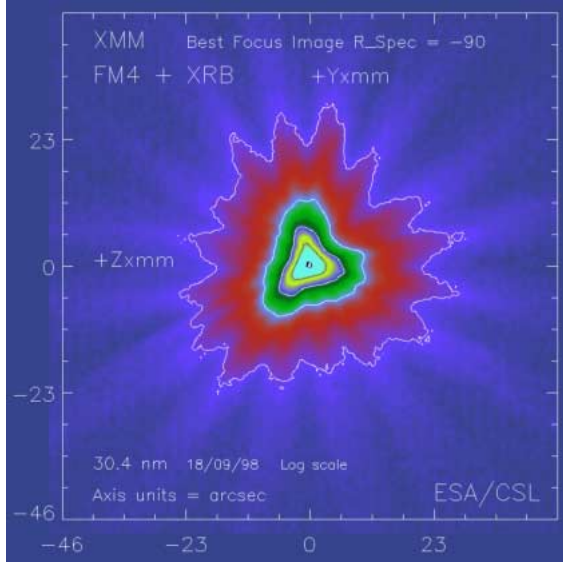


Figure 3.b : EUV PSF at 30.4 nm with RGA

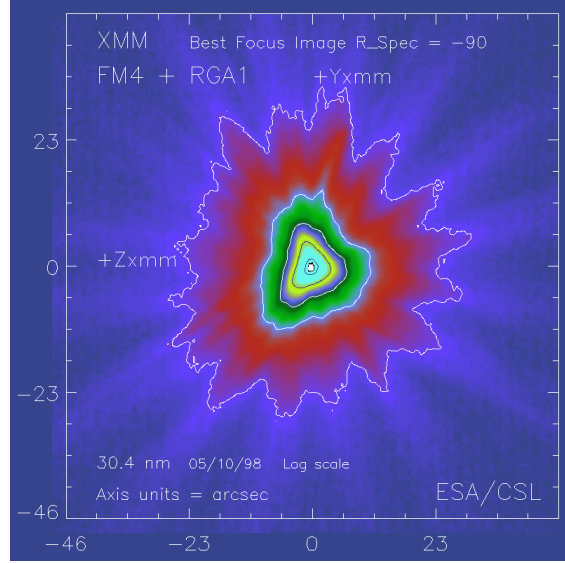
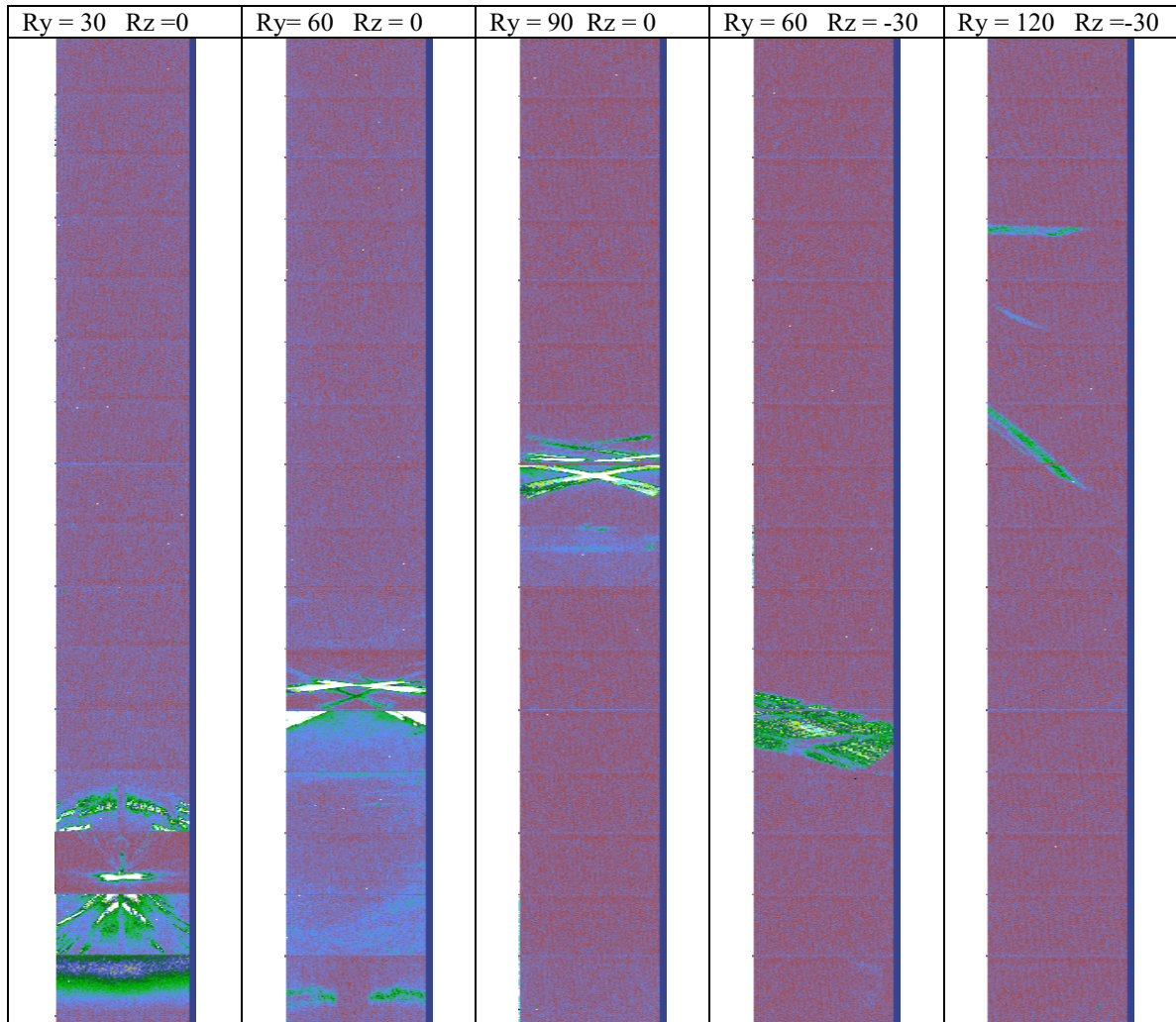


Figure 4 : Unfocused stray light on RFC for off axis angles (Not to scale)



Evaluation of focused and unfocused stray light in RGA Focal Camera (RFC) area was also performed, as well. Therefore, the RFC area is covered by 16 EUV CCD in line. Samples of stray light images on RFC are presented in figures 4. EUV focused stray light at 0-order focus is also evaluated in terms of effective area and gives results similar to the FM4 MM+ RGA2 combination.

4. FM5 MM EUV TESTING

FM5 MM was delivered in early 1999 and was subjected to the complete set of environmental and optical tests at CSL. When the first reference optical test was performed it was immediately clear that the FM5 MM was by far the best MM. After each environmental test an optical test was performed taking 5 days including the integration and alignment tests. The environmental tests did not cause any degradation to the optical quality of the MM confirming the results of the previous MM tests. On completion of the test at CSL FM5 has been sent to MPE for X-ray effective area calibration. A summary of the main results of CSL tests are presented below.

EUV tests

Figure 5 summarises the evaluation of the Point Spread Function (PSF) for all the MMs built. The HEW calculated from EUV best focus PSF at 58.4 nm gives 11.7 arcsec as compared with the 14.1 arcsec for FM4 MM. It should be noted that this is a significant improvement in the optical performance and confirms the trend of the XMM Mirror Module production during the project development. The main contributions to this improvement are due to advances in the MS manufacturing process and the integration alignment procedure. The MS used for FM5 have been manufactured with a more advanced technique that has enabled a better control of the focal length. This result in a MM with the mirrors more closely matched in terms of focal length and consequently generating a smaller focus blur in the best focus plane. In addition, the alignment has been continuously improved to reduce dispersion in the MS centring.

Figure 5 : HEW, 90EW and FWHM at best focus for all the tested MM

<i>MM model</i>	<i>QM</i>	<i>FM1</i>	<i>FM2</i>	<i>FM3</i>	<i>FM4</i>	<i>FM5</i>
HEW in arcsec	19	15.5	15.4	14.1	14.1	11.7
90EW in arcsec	79	62.6	62.5	59.2	63.1	53.1
FWHM in arcsec	11	6.7	6.3	4.5	4.8	4.5
Focal length in mm	7494.6	7493.0 +/- 0.5	7493.2 +/- 0.5	7493.6 +/- 0.5	7493.4 +/- 0.5	7494.5 +/- 0.5

The extra focal image shows the same behaviour as for the other FM MMs, the 16 spokes are clearly identified and the annular shape is circular with some small local defects present that indicate possible deformation close to the MS interface with the spider. The azimuthal intensity distribution between each sector in the extrafocal images has variation less than 1 % RMS, demonstrating the uniformity of the image.

A simplified stray light test confirmed that there was no “ghost image” as experienced during the previous FM MM stray light tests⁵. This ghost image was a ring that crossed the middle of EPIC detector when a MM was tilted to an angle of 30 arcmin. No numerical model had foreseen this as a stray light contribution.

The PSF in the FOV was also measured between -15 to + 15 arcmin (the EPIC FOV). For rotation around Z_{xmm}, the maximum throughput and the minimum HEW are close to each other (the difference is about 6 arcsec), limited by the measurement accuracy. During rotation around the satellite Y axis a difference of 105 arcsec is observed. For this azimuth the maximum throughput is not aligned with respect to the minimum HEW. This behaviour is observed on all the MMs. Some explanations of this behaviour will be developed latter, using the result of MS11 testing.

Figure 6 : EUV best focus PSF at 58.4 nm. The 3-D view PSF is in log scale. The central core is thin and rises very fast compared to the previous FM MM

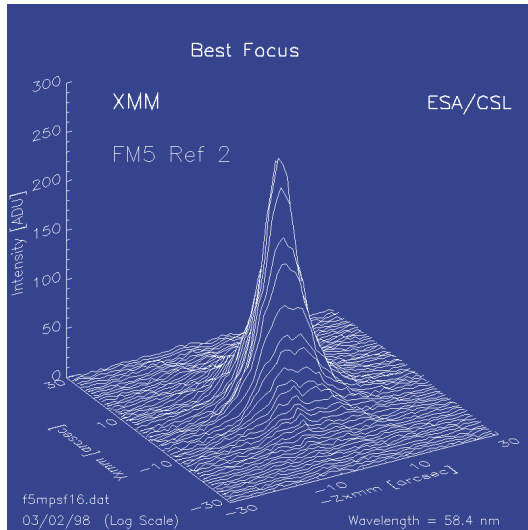
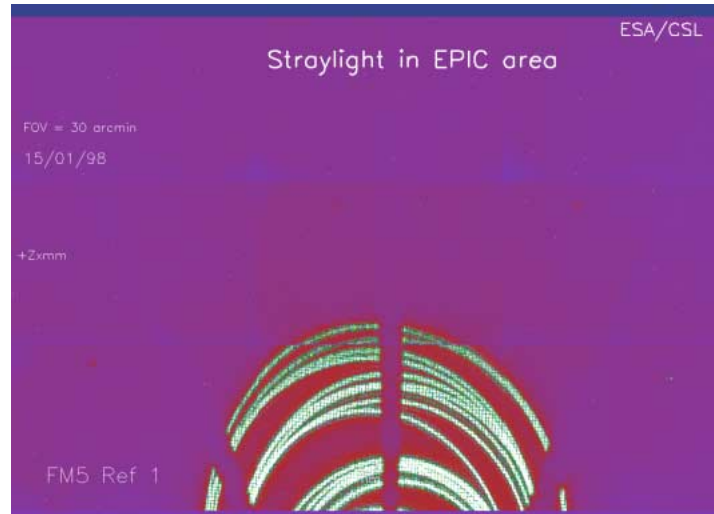


Figure 7 : Stray light in Epic area for a source at 30 arcmin. The image is the one expected from numerical simulation. The central part of the field is free of “ghost image”.



X-ray test

X-ray pencil beam tests were performed in order to measure the effective area⁹ of the XMM FM5 MM. This technique measures the reflectivity of each MS along one azimuth in a finite area. The measured value is corrected for known loss by scattering and is multiplied by the geometrical area of the respective MS. The resultant effective area values for 3 optical tests (Ref 1, 2, 3), are given in figure 8 together with the measured value at EUV energy (0.021 keV). At this wavelength a loss of 15 % is observed as on all the previous MM FM; probable causes of this are discussed later in § 5.

After each environmental test the effective area has been measured (table of figure 8, Ref 1, 2 and3) with the pencil beam technique and the repeatability of the results is within 4%. Repeat test using a different azimuthal position gave a variation of 2 % at most. The effective area results calculated from pencil beam measurements were compared to measurements achieved with other methods and in another facility⁹. A deviation of less than 4 % peak to valley was observed with the absolute value. The achieved results on FM5 MM are comparable to the ones achieved with FM4 MM (average over 2 measurements). These results have still to be confirmed by the MPE X-ray calibration.

Measurement of wing scattering at higher energies using a Au target with an Al filter was considered but was discovered to be beyond the sensitive range of the X-ray CCD.

Figure 8 : FM5 MM effective area in EUV and in X-ray using pencil beam reflectivity data

Effective area [cm ²]	FM4	FM5 Ref 1	FM5 Ref 2	FM5 Ref 3 Az 0° / Az 180°
Energy in keV	Average of 2	First test	After vibration	After thermal test
0.021	1530	1511	1527	No reliable result
1.5	1417	1385.54	1365.27	Not Performed
2.1	1263	1207.26	1218.16	1240.3 / 1233.4
2.29	882	852.62	863.09	Not Performed
8	596	572.08	563.9	582.6 / 587.1
8.9	476	438.44	453.84	457.6 / 465.1
9.7	355	340.77	344.31	352.5 / 360.9
11.5	163	157.87	158.26	166.8 / 170.9

5. MEASUREMENTS OF SINGLE MIRROR SHELL N° 11 OF FM5

The purpose of the tests was to evaluate the optical performance of an integrated single MS. The results enable:

- cross correlation with the integration optical bench and other metrology measurements
- to better understand effects of the integration process
- to observe the individual mirror performance with respect to the mirror module results.

The test was conducted directly after the FM5 MM environmental and optical tests. Selection of the single mirror shell 11 was made by means of an aperture stop integrated on the RGA interface, 256 mm behind the mirror. To enable comparison with the complete MM, the alignment corresponding to the maximum throughput versus the collimator beam was maintained. In this configuration the difference with respect to the mechanical axis (alignment lens axis) is 20 arcsec. The main tests carried out were EUV, however a test using the X-ray pencil beam was also performed.

EUV tests

During the alignment of the aperture stops, the hyperbola focus of the MS was observed. It was noticed that there was a mis-alignment of the hyperbola axis with respect to the MM optical axis. The observed tilt was calculated to be -1.1 arcmin around Z axis and -0.65 arcmin around Y axis. This result was supported by later measurement using the MS11 PSF HEW variation versus FOV, where the minimum HEW is achieved for -1.8 arcmin and 0.2 arcmin. This behaviour is also observed on the complete MM (difference between the maximum throughput and the minimum HEW axis) as presented previously. These results suggest that the observation of the hyperbola focus, as used in the integration process, provides a useful diagnostic tool and that the integration process could benefit by the application of the PSF quality.

It should however be noted that due to the mandrel, from which the mirrors are replicated, the optical axis of the hyperbola is not necessarily perfectly aligned with the parabola one and consequently with the mirror shell as a whole. Therefore to accurately use the hyperbola focus method for the alignment, mandrel data are also required to be taken into account.

In practice some difficulty in the measurement was experienced due to the position of the aperture stop which, for simplicity of design, was placed on the RGA interface some distance behind the mirror shell. It was noted that it was possible for reflected light to come from some of the other mirror shells and to reach the MS11 hyperbola focus. Potential effects of this on the measurements made could not be fully evaluated. Secondly, the laser beam is not perfectly homogeneous and therefore is not easy to find the optimum alignment using only the hyperbola focus.

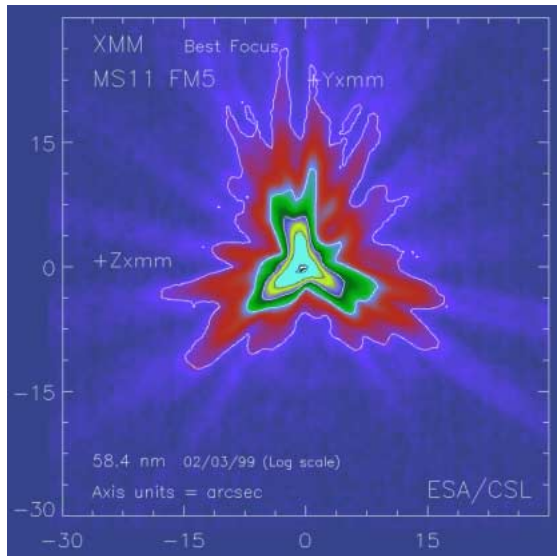
The measured focal length of the single mirror shell is identical to the one of the complete MM. This is confirmed by the focal length measured at Media Lario. The measurements performed by the Vertical Optical Bench and the calculated best focus of the mirror module in optical light, showed in fact a MS focal length 1.2 mm shorter with respect to the average focal length of the MM, which is a value within the accuracy of the measurement.

Analyses of extra focal images at the Vertical Optical Bench at Media Lario are limited by diffraction (figure 10.a). This limits the diagnostics on what happens at interface points between spider and MS. The EUV extra focal image (figure 10.b) shows clearly a local deformation of the MS at each spider interface. This behaviour is present in best focus PSF following symmetry of 16. These impacts are not integrated in the SCISIM model^[10,11], and therefore the effect of the spider is not seen in the simulated images. SCISIM model is a numerical model of XMM, built from all the MS metrological data available before integration of the MS on the spider.

Measurements of the effective area of a single MS presents the same missing fraction as the complete MM (see table of figure 8). Possible reasons for this may be:

- Irregular geometry of the MS has been observed in the experimental measurements but has not been fully integrated in the models.
- The measurement inaccuracies, evaluated to 3 % RMS.
- Lack of reliable information on gold reflectivity at 58.4 nm for grazing angle. No actual measurement has been performed on a sample.
- Possible molecular contamination (hydrocarbons are a well-known source of reflectivity loss in the EUV range) and particle contamination that can cause vignetting in the EUV, but not necessary in the X-ray due to the higher penetration of the radiation.

Figure 9 : EUV PSF at 58.4 nm of FM5 MM integrated MS11



Best focus PSFs show interesting features.

First the image is triangular in the same directions as the PSF of the whole MM and clearly representative of this type of deformation.

Close inspection shows that the corners of the triangle have a fork shape indicating that the points are aligned with the MIS interface fixations with the spacecraft.

The 3-points deformation is typically the behaviour of the simulated PSF performed on a MS deformed by a twist of the spider. These deformations were studied by finite element, and have been implemented in the SCISIM simulator. From this analysis, it appears that for future X-ray missions the design of the spider has to be optimised in order to reduce deformations and enable a proper use of high quality MS. The integration process of the Mirror Interface Structure to the spider needs also to be further optimised. Indeed images in optical light before the MIS integration show better symmetry.

Figure 10.a : Combined focus extra focal in the visible (633nm) on the Media Lario Vertical Optical bench.

This image is used for MS alignment using a Hartman test. The spider diffraction can be observed in the lines radial to the circle. The concentric rings correspond to the MS diffraction. All these rings contribute to a central point that is more intense.

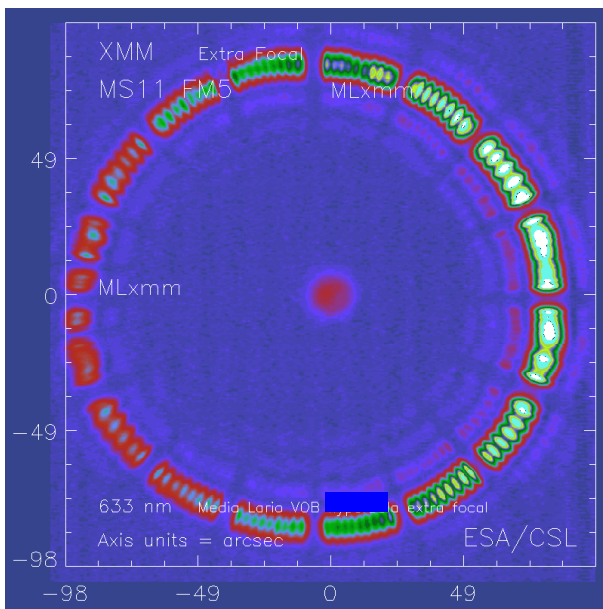
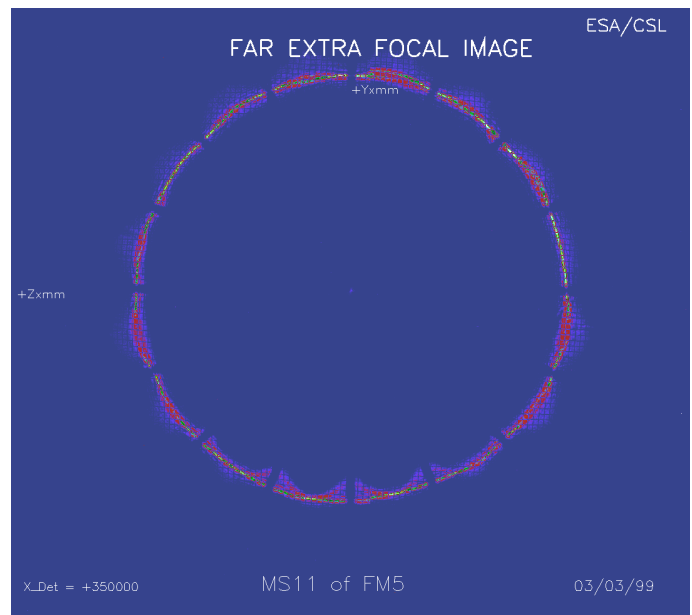


Figure 10.b : Telescope extra focal in the EUV with the CSL vertical facility.

The grid observed on the images comes from the Al filter mesh. The large rings on the bottom confirm that the MS is slightly tilted. The rings can be equalised by tilting the MM. For far extra focal images the figure presents good circularity. Close extra focal images indicate a triangular shape.



X-ray tests

X-ray pencil beam tests were performed to evaluate the slope error of the MS. The method used is to translate the MS 11 in front of the pencil beam in an azimuthal direction. The detector moves synchronously with the MM. In the ideal situation, the spot should stay at the same position on the detector. Any deviation from this position should indicate an axial slope error of the double reflection on the mirror shell scanned azimuth.

From the middle of the MS 11, stepping of 200 μm (of the MM and the CCD detector) were performed until no more signal was recorded on the CCD. The position of the centre of the spot is recorded for each step, and a graph of the deviation from the nominal position versus the MS position is plotted. From this data, the deviation in μm can be translated in arcsec slope error of the two reflections. A deviation of the double reflection was observed at telescope focus. As a first approximation, assuming that the parabola and hyperbola section are straight lines (figure 11), the slope angle is given by $\Delta x / (4 * \text{focal length})$, where Δx is the deviation from nominal position and f the focal length. The plot of figure 11 presents the 'combined' axial slope error for an azimuth at 5 degrees in between spoke 9 and 10 using previous approximations. This measurement was also repeated at the middle between Spoke 1 and 2. The achieved results are within the expected slope error.

Analysis of results must take into account the following factors:

- The slope error measured is the result of both parabola and hyperbola reflection. Therefore the final measurement contains two main contributions: slope errors due to local deformations of the mirror shell and errors due to mismatch of the parabola and hyperbola alignment. These errors are linked both to the mandrel and to the mirrors production process.
- Measurements made show a peak slope error at the interface plane. From other types of measurement performed during mirror shell production and integration it is well known that the zones most likely to have a slope error are at the ends of the mirror shell. Further investigations on this subject are therefore planned for the future.

Figure 11. : Axial slope error approximation deduced from the spot deviation in the telescope focal plane.

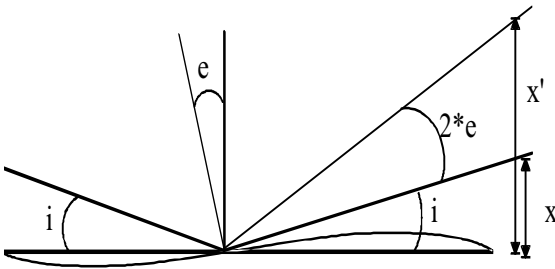
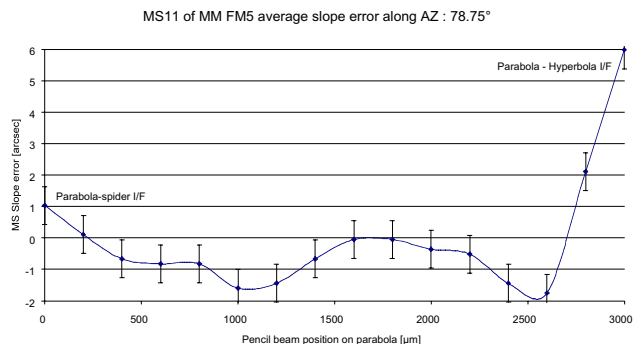


Figure 11 : Axial slope error for an azimuth at 5 degrees from spoke 9, between spoke 9 and 10



Possible improvements to the measurement technique could be measurement of the slope error of the hyperbola section by tilting the MM (about 34 arcmin) in such a way that incoming X-ray beam is parallel to the parabola. In this case the detector has to be located at hyperbola focus. Knowing the hyperbola slope error and the whole MS one, the parabola slope error can be deduced. This is possible if the inner MS is not yet integrated, otherwise the parabola shadows the hyperbola section.

6. LESSONS LEARNT

Many lessons have been learnt during these last 5 years of facility development, operation, MM manufacturing and testing. They are already summarised in ref 12. Through the XMM project significant steps forward have been made in the very specialised field of X-ray optics. Every single phase and any piece of work done in these years has been taken by the project team as a new challenging opportunity to progress in the scientific and technological field. Now, after the very promising performance reached by the Mirror Modules produced so far, all future developments look to the future of X-ray astronomy and the next generation of X-ray telescopes.

Data collected so far indicates that the nickel replication technology used for the production of the XMM mirrors has not yet been exploited to the limits. The programme was started from little more than the knowledge of a technique in 1994. A new dedicated manufacturing facility was set up and in the space of two years a Qualification Model MM demonstrated the capabilities of this technology to achieve a HEW of 19 arcsec at Mirror Module level. Now, in 1999 five flight models have been built and space qualified, reaching a HEW on the last MM of 11.7 arcsec. This value is far better than the project's original requirements, demonstrating the achievements that can be made by small dedicated teams.

The EUV tests have the major advantage to illuminate properly the MS and to avoid diffraction and scattering. This allows to achieve good knowledge of the impact of the mid and low frequency surface errors on the PSF. The conclusions drawn by the EUV tests show that the sources of these surface errors are clearly identified and will be discussed hereafter. Concerning the high frequency surface errors that cause scattering it is well known that it is necessary to have super polished surfaces. Through the XMM project the capability of the electroforming technique to replicate a mirror keeping the same surface roughness of the master has also been demonstrated. This has been verified by local measurements of micro roughness or angle resolved scattered measurements. The RMS micro roughness achieved on the XMM MS is the same as the one specified for the mandrels and it is in average 4 Å, but some MS in some areas are close to 2 Å. An average value of 2 Å, which is something desirable for future development, can only be achieved by improving the mandrel quality.

The important features from these last EUV measurements are summarised hereafter:

The focal length of the individual MS is the same as the one of the MM. At Media Lario the MS11 measured focal length is 7497.6 mm compared with 7498.8 mm for the MM. Future improvements should concentrate on the following aspects:

- focal length calibration of the integration optical bench
- improvement of the mandrel
- improvement of MS to get the correct focal length

The expected improvement in terms of MM HEW, which can be obtained optimising the above points, is evaluated to be about 1 arcsec. Moreover some efforts have to be put on other factors degrading the MM image quality which could bring a more significant contribution to possible improvements. In particular the stresses induced on the mirrors by the spider and the MIS. These cause two main effects:

- The triangular shape in the focal image which is due to the spider torsion caused by the interfacing of the MIS to the spider. Stiffening or modifying the spider and MIS design could reduce this effect.
- Local out of roundness of the mirrors.

This is linked to the gluing points between the MS and the spider. A lot of care is already taken during this procedure and it is not sure if strain is induced by the gluing process or later forces applied to the spider. Future testing should be addressed to this point.

The expected improvement coming from these last aspects can be evaluated as follow. MS 11 HEW is measured at Media Lario to be of 6 arcsec. This value is obtained by 3 different methods: screening device (6.87 arcsec), Vertical Optical Bench (5.7 arcsec) and MS visible PSF deconvolution (6 arcsec). At CSL the measured value is 9 arcsec. The focal image shapes are however quite different. The main difference in the measurement supporting system is that at Media Lario the MM is supported by the spider (MIS integrated) while at CSL the MM is supported by its spacecraft interfaces. In the latter case the supporting system may increase the triangular shape in the PSF. Therefore the discrepancies between the two HEW figures are not only linked to the measurements techniques but also to the supporting systems. To confirm this assumption, cross check tests could be designed and performed at both facilities using both types of supporting interface. In this case, an improvement of 3 arcsec (9 arcsec (CSL) - 6 arcsec (ML)) could be achieved on each MS, and by this way on the complete MM by improving the supporting system.

The X-ray pencil beam showed local axial slope errors. By reducing them the final PSF will be also reduced.

These elementary analyses show that a MM with a final HEW about 6 arcsec might be very likely produced even without introducing main conceptual changes in the production process.

7. CONCLUSIONS

This paper has summarised the results of the last tests performed on XMM MMs at CSL. It had shown that the FM4 MA flight configuration is ready for its integration on the payload. Its optical quality is comparable to the FM3 MA, which includes also a Reflecting Grating Assembly (RGA). A fifth flight model was manufactured and tested. This provides the project a spare Mirror Module of the highest quality. As XMM is planned to be launched before the end of this millennium it is unlikely that the FM5 MM will be integrated on the spacecraft. However, this last Mirror Module has provided a

perfect opportunity to further advance the MM production technique reaching a final performance of 11.7 arcsec HEW and showing that the nickel replication technology for manufacturing X-ray optics has not yet been exploited to the limits. Moreover, the powerful analysis tools developed at CSL have provided useful data, complementary to the ones available from the mirrors production and integration. The advantage of the EUV collimated beam is to illuminate with a perfect parallel beam the MM and the use of EUV wavelength makes the diffraction and the scattering effects negligible. This allows to focus all the analysis on shape surface errors, which remains the more critical ones as the high frequency surface errors are now very well controlled during the production process and can be measured on each shell before integration. Through the analysis of all the available data, possible area of improvements for the future have been identified and the nickel electroforming technology proves to be very promising for coming X-ray applications.

Acknowledgements

The authors wish to thank the test teams who at the moment of greatest need worked hard 24 hours a day, 7 days a week to complete these tests.

Many thanks go also to the manufacturing teams for their valuable, persevering and accurate work. Without them, no MM of this quality will ever be built.

The vertical facility was funded by ESA XMM project under the ESTEC contract number 9939/92/NL/PP. The XMM MM mirrors were replicated and integrated by Media Lario S.r.l. (Bosisio Parini – Italy) under ESA contract number 0545/93/NL/RE. The X-ray Baffle was developed by SENER (Las Arenas Spain) and DORNIER under ESA contract number 11860/96/NL/RE. The development of RGA grating arrays is supported by NASA under contract of the University of California at Berkeley with subcontracts to Columbia University and Lawrence Livermore National Laboratory.

References

1. D. Lumb, H. Eggel, R. Lainé, A. Peacock, "X-ray Multi-Mirror Mission - an overview", SPIE Conference 2808-32, Denver 1996.
2. D. de Chambure, R. Lainé, K. van Katwijk, J. van Casteren, P. Glaude, "The Status of the X-ray Mirror Production for the ESA XMM Spacecraft", SPIE Conference 2808-35, Denver 1996.
3. J.Ph. Tock, I. Domken, J.P. Macau, Y. Stockman, M. Thomé, J. Jamar, Ph. Kletzkine, "Status of XMM Test Programme in CSL EUV and X-ray Test Facility (FOCAL X)", First XMM Workshop at ESTEC, Noordwijk 1998
4. Y. Stockman, J.P. Collette, J. Ph. Tock, D. de Chambure, Ph. Gondoin, "Optical testing of XMM Flight Module I and II at the vertical EUV/X facility", SPIE San Diego 1997.
5. Y. Stockman, I. Domken, H. Hansen, J.Ph. Tock, D. de Chambure, Ph. Gondoin, "XMM Flight Mirror Modules Environmental and Optical Testing", SPIE, San Diego 1998.
6. Y. Stockman, I. Domken, H. Hansen, J.Ph. Tock, T.A. Decker, A. Rasmussen, A.J.F. den Boggende, J.W. den Herder, F. Paerels, G. Bagnasco, D. de Chambure, C. Erd, Ph. Gondoin, "XMM Flight Mirror Module with Reflection Grating Assembly and X-Ray Baffle Testing", SPIE, San Diego 1998.
7. D. de Chambure, W. Ruehe, D. Schink, E. Hoelzle, Y. Gutierrez, M. Domingo, I. Ibarretxe, J.Ph. Tock, I. Domken, Y. Stockman, Y. Houbrechts, H. Hansen, B. Aschenbach, "The X-Ray Baffle of the XMM Telescope : Development and Results", International Symposium on Optical Systems Design and Production, Berlin 1999.
8. D. de Chambure, R. Lainé, K. van Katwijk, "The X-Ray Telescopes for ESA XMM Spacecraft", SPIE vol 3444 pg 313- 326.
9. Y. Stockman, H. Hansen, Y. Houbrechts, J. Ph. Tock, D.de Chambure, P. Gondoin, "XMM Flight Mirror effective area", International Symposium on Optical Systems Design and Production, Berlin 1999.
10. Ph. Gondoin, B. Aschenbach, M. Beijersbergen, R. Egger, F. Jansen, Y. Stockman, J.P. Tock, "Calibration of the first XMM Flight Mirror Module I - Image quality ", SPIE 3444 , San Diego 1998.
11. Ph. Gondoin, B. Aschenbach, M. Beijersbergen, R. Egger, F. Jansen, Y. Stockman, J.P. Tock, "Calibration of the first XMM Flight Mirror Module II - Effective area", SPIE 3444 , San Diego 1998.
12. D.de Chambure, R. Lainé, K. van Katwijk, P. Kletzkine, A. Valenzuela, G. Grisoni, M. Canali, S. Hofer, D. Kampf, JP. Tock, I. Domken, H. Hansen, M. Léonard, Y. Stockman, B. Aschenbach, H. Brauninger, "Lessons Learnt from the development of the XMM optics", International Symposium on Optical Systems Design and Production, Europto, Berlin 1999.